A state-of-the-art anisotropic rock deformation model incorporating the development of mobilised shear strength

M J Md Noor[1] and A F Jobli[2]
[1] Faculty of Civil Engineering, Universiti Teknologi MARA, 40450 Shah Alam, Selangor, Malaysia
[2] Faculty of Civil Engineering, Universiti Teknologi MARA, 94300 Kota Samarahan, Sarawak, Malaysia

E-mail: ahmad151@sarawak.uitm.edu.my

Abstract. Currently rock deformation is estimated using the relationship between the deformation modulus E_m and the stress-strain curve. There have been many studies conducted to estimate the value of E_m. This E_m is basically derived from conducting unconfined compression test, UCS. However, the actual stress condition of the rock in the ground is anisotropic stress condition where the rock mass is subjected to different confining and vertical pressures. In addition, there is still no empirical or semi-empirical framework that has been developed for the prediction of rock stress-strain response under anisotropic stress condition. A rock triaxial machine GCTS Triaxial RTX-3000 has been deployed to obtain the anisotropic stress-strain relationship for weathered granite grade II from Rawang, Selangor sampled at depth of 20 m and subjected to confining pressure of 2 MPa, 7.5 MPa and 14 MPa. The developed mobilised shear strength envelope within the specimen of 50 mm diameter and 100 mm height during the application of the deviator stress is interpreted from the stress-strain curves. These mobilised shear strength envelopes at various axial strains are the intrinsic property and unique for the rock. Once this property has been established then it is being used to predict the stress-strain relationship at any confining pressure. The predicted stress-strain curves are compared against the curves obtained from the tests. A very close prediction is achieved to substantiate the applicability of this rock deformation model. This is a state-of-the art rock deformation theory which characterise the deformation base on the applied load and the developed mobilised shear strength within the rock body.

1. Introduction

Progressive slow deformation in rock structure will result in catastrophic failures and therefore rock deformation modelling is important as it helps to predict future deformation for stability of any foundation or infrastructure. It is generally known that the strength of rock also plays an important role in the multi-peak deformation behavior of rock mass. Both strength and deformability of fractured rock masses are important factors in the design and construction of civil and mining structures [1]. The importance of obtaining not only the peak strength but also the complete stress–strain curve of rocks by conducting laboratory tests has also been recognized as it could affect rock stability [2]. Up to date, there are a competitive number of researchers focusing on rock strength deformation model. However, most of them had excluded the role of confining pressure in their rock deformation model like the model introduced by Cheng et al [3], Korneva et al [4] and Xue et al [5]. Some of the researchers perform numerical simulations to assess failure behavior and reconstruct rock deformation as

conducted by Wang et al [6] and Li et al [7]. However, the design parameter and simulations is found to be troublesome due to its complexity.

This paper introduces a new rock deformation model, which incorporate the build-up mobilised shear strength within the rock body during the application vertical loading. In fact this model is based on the interaction between role of strength and the applied load in characterizing the rock deformation. The prediction framework utilizes the non-linear shear strength envelopes introduced by Md Noor et al [8-9]. This model is based on the rock true stress-strain curves.

2. Laboratory rock triaxial test

The stress-strain curves of the test rock specimen are obtained using rock triaxial machine, GCTS Triaxial RTX-3000 which uses GCTS CATS software to run the test. The test specimens are in the form of cylindrical specimen of 50 mm diameter and 100 mm height. The test rock is weathered granite grade II, which obtained from site within Rawang by deep boring work at depth of 20 m. The placement of the test specimen in GCTS Triaxial machine is shown in Figure 1 while Figure 2 shows a schematic diagram of the overall set up. The procedure of triaxial testing followed the standard GCTS CATS software.

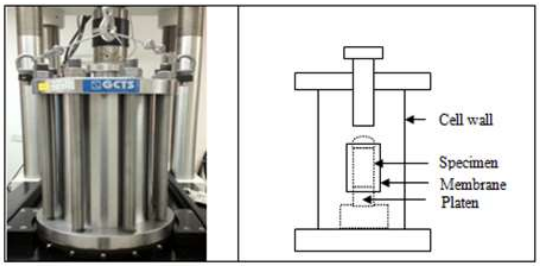

Figure 1. Installation of rock specimen into GCTS RTX-3000 Triaxial machine

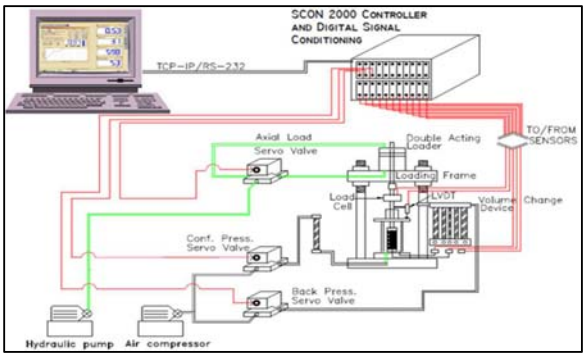

Figure 2. Schematic diagram of GCTS RTX-3000 Triaxial machine set up

The RTX-3000 GCTS triaxial machine capable of applying different confining pressures which may be varied from 0 MPa to 150 MPa. As mention by Hoek and Brown [10], the maximum confining pressure can be applied is up to 50 % of maximum compressive strength. However in this study, the rock specimens were only subjected to three confining pressures which are 2 MPa, 7.5 MPa and 14 MPa. The application of deviator stress is at a constant rate of 0.01% strain. This is to suit the time of failure to be within 5 to 20 minutes. Figure 3 then depicts the stress-strain curves of the test rock at the different confining pressures.

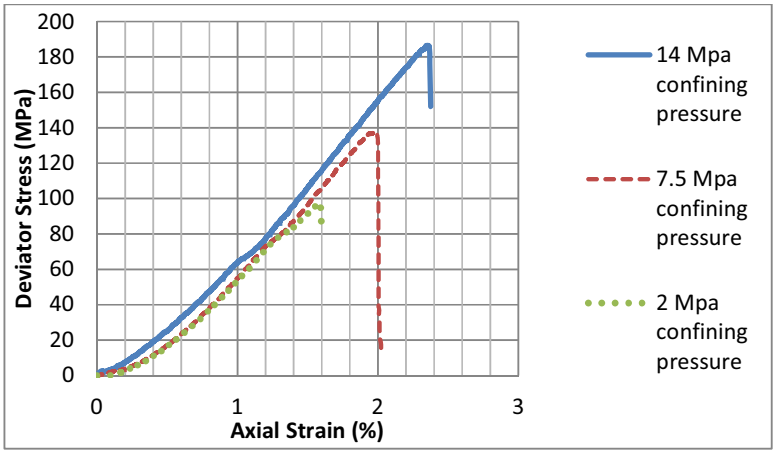

Figure 3. Stress strain curve of weathered granite at different confining pressure

3. Shear strength envelope at failure and normalise stress-strain curves

During the shearing stage in the triaxial tests, the specimens undergo axial compression and subsequent lateral expansion. This condition is called anisotropic stress condition whereby the vertical and the lateral stress are not equal. The lateral pressure is contributed by the applied cell pressure while the vertical pressure is the sum of the applied deviator stress and the applied cell pressure. The deviator stresses at failure for the tests at confining pressures of 2 MPa, 7.5 MPa and 14 MPa are 97.26 MPa, 137.89 MPa and 186.54 MPa respectively. These values are used to plot the shear strength envelope at failure as shown in Figure 4.

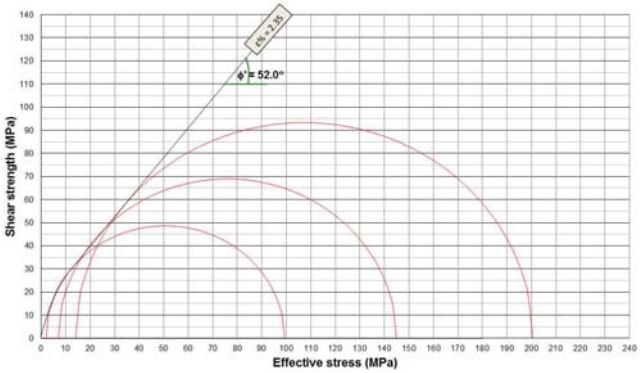

Figure 4. Shear strength envelopes at failure (ε = 2.35%)

Based on Figure 3, since the failure occurs at different axial strain which are 1.58%, 1.98% and 2.35% for confining pressure of 2 MPa, 7.5 MPa and 14 MPa respectively, then a normalize stress strain curves is needed in order to plot the development of the mobilised shear strength envelopes during the application of the deviator stress. The normalised stress-strain curves are obtained by multiplying the respective axial strains with respective normalise factor so that the peak failure deviator stresses is shifted to coincide with the maximum failure axial strain of 2.35%. The normalise conversion factors are 1.482 and 1.186 for the confining pressures of 2 MPa and 7.5 MPa respectively and they are calculated using Equation 1. The normalised stress-strain curves are as shown in Figure 5.

$$\text{Normalise conversion factor} = \frac{\text{Maximum axial strain (\%) at failure}}{\text{Axial strain (\%) at failure under consideration}} \quad (1)$$

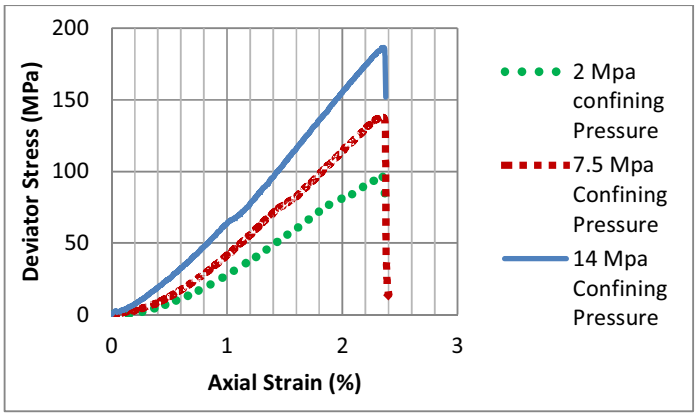

Figure 5. Normalise stress-strain curve for different confining pressure

4. Axial strain and shear strength interaction as the inherent property of the test rock

The mobilised shear strength envelopes are plotted for axial strains from 0.2% to 2.35% at increment of 0.2%. The corresponding mobilised shear strength envelopes at different axial strains are then presented in Figures 6(a), 6(b) and 6(c). The mobilised shear strength envelopes for all axial strain then are presented in Figure 7. These mobilised shear strength envelopes are considered as the inherent property of the test rock, and will be utilized for the prediction of deviator stress under any confining pressure. Whenever the rock specimen is compressed by applying the deviator stress the rock mass automatically resists the compression through the build-up mobilised shear strength developed within the rock mass. Therefore, the mobilised shear strength is taken as the deformation resisting variable in this theoretical rock deformation model.

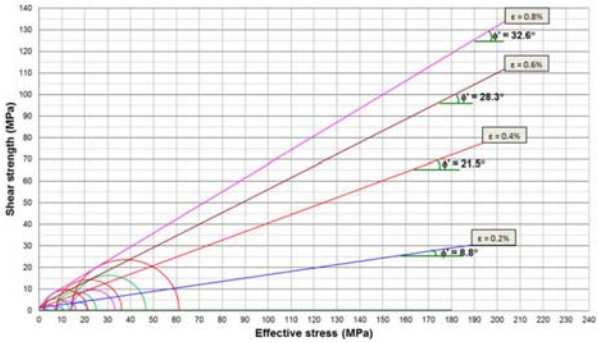

Figure 6(a). Mobilise shear strength envelopes for axial strains of 0.2, 0.4, 0.6 and 0.8%

The applied anisotropic stress to the specimen is defined by the Mohr circle. When the deviator stress is increased, the diameter of the Mohr circles grows bigger and the Mohr circle extends beyond the current mobilised shear strength envelope. This is a state of in-equilibrium and the rock mass automatically developed a higher mobilised shear strength. This is indicated by the mobilised shear strength envelope rotating anti-clockwise about the origin to mark the increase. Whenever the envelope reinstates the touching of the Mohr circle, then the state of equilibrium between the applied pressure and the developed mobilised shear strength is achieved. This process repeats continuously until the shear strength envelope at failure is arrived. Different rock would have a different distribution

of mobilised shear strength envelopes and the shear strength envelopes at failure. Therefore, these mobilised shear strength envelopes and the shear strength envelopes at failure is the unique property of the rock itself.

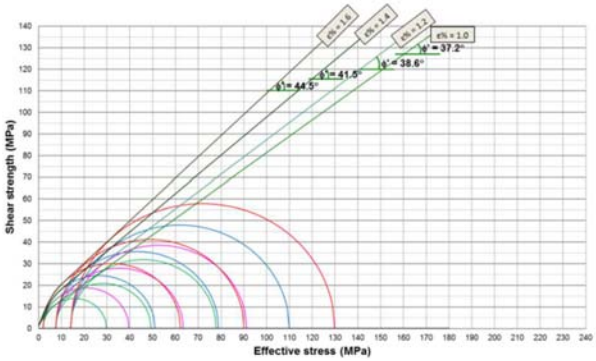

Figure 6(b). Mobilise shear strength envelopes for axial strains of 1.0, 1.2, 1.4 and 1.6%

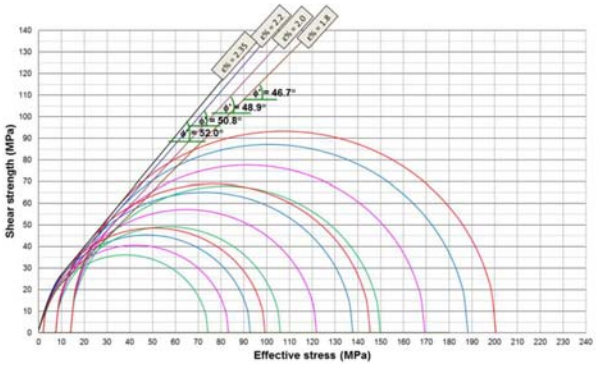

Figure 6(c). Mobilise shear strength envelopes for axial strains of 1.8, 2.0, 2.2 and 2.35%

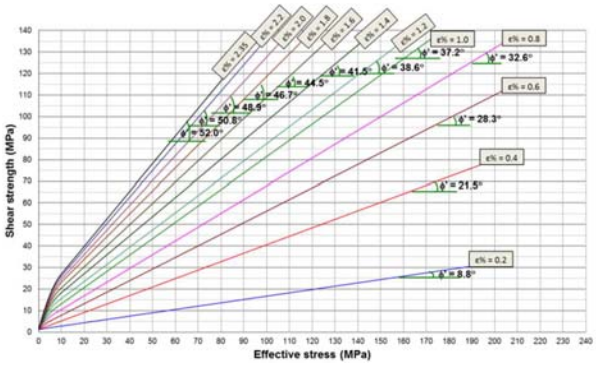

Figure 7. A complete mobilise shear strength envelopes of the test rock for 0.2% to 2.35% at increment of 0.2%

5. Prediction of stress-strain response

Since the mobilised shear strength envelopes obtained in Figure 7 is the inherent properties of the test rock, then this property is valid for any stress range. Therefore this mobilise shear strength envelopes can be applied to predict the stress strain response of the test rock at any confining pressure. Thus in order to check the validity of this assumption, the stress-strain response at confining pressure of 2 MPa, 7.5 MPa, and 14 MPa are predicted by drawing the Mohr circles with the volume of σ_3 as the minor principle stress which is equals to the applied confining pressure. The Mohr circles are drawn to touch the respective mobilised shear strength envelopes and the diameter of the Mohr circle represent the corresponding deviator stress as shown in Figure 8a, 8b and 8c respectively.

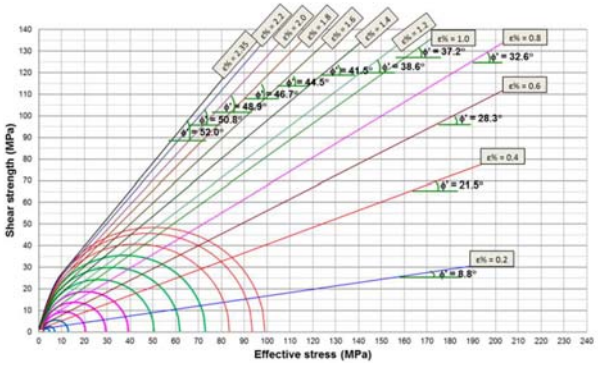

Figure 8(a). Deviator stress prediction at 2 MPa confining pressure

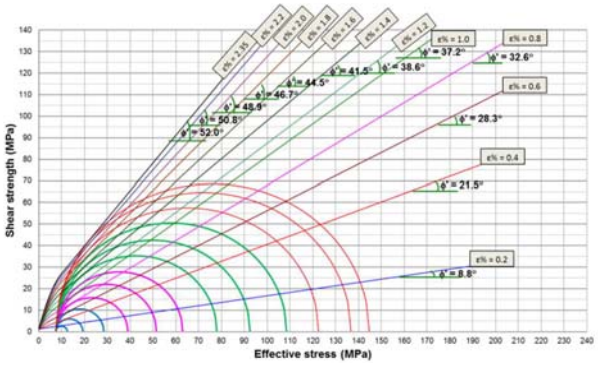

Figure 8(b). Deviator stress prediction at 7.5 MPa confining pressure

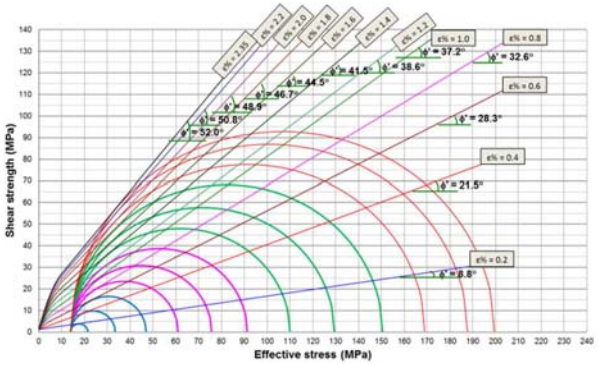

Figure 8(c). Deviator stress prediction at 14 MPa confining pressure

The complete drawing of Mohr circles from Figure 8 now enables the prediction of the deviator stress. The values of the predicted deviator stresses corresponding to the respective normalised axial strain is shown in Table 1. In order to compare the prediction of the stress-strain curves to the actual experimental results, the normalised strain need to be multiply by the inverse factor to represent the corresponding stress to the respective axial strain. The inverse factors are 0.675 and 0.843 for the confining pressures of 2 MPa and 7.5 MPa respectively and they are calculated using Equation 2. The complete prediction of stress-strain values are presented in Table 2. Figure 9 then depicts the predicted stress-strain curves plotted superimposed on the actual laboratory stress-strain curves.

$$\text{Normalise inverse factor} = \frac{\text{Axial strain (\%) at failure under consideration}}{\text{Maximum axial strain (\%) at failure}} \quad (2)$$

Table 1. Magnitudes of the predicted deviator stress

Normalised axial strains (%)	Predicted Deviator stress (MPa) i.e diameter of Mohr circles		
	2 MPa confining pressure	7.5 MPa confining pressure	14 MPa confining pressure
0.2	2.8	5.0	7.5
0.4	5.0	11.8	19.5
0.6	11.0	21.0	33
0.8	18.5	31.5	47
1.0	27.4	44.0	61.7
1.2	37.3	55.5	77.3
1.4	48.5	70.5	96
1.6	59.8	85.0	115.4
1.8	71.0	101.0	136.5
2.0	81.5	115.0	155
2.2	91.5	129.2	173.7
2.35	97.0	137.2	185.5

Table 2. Prediction of the stress-strain values

Normalised axial strains (%)	2 MPa confining pressure		7.5 MPa confining pressure		14 MPa confining pressure	
	Predicted deviator stress (MPa)	Inversed axial strain (%)	Predicted deviator stress (MPa)	Inversed axial strain (%)	Predicted deviator stress (MPa)	Inversed axial strain (%)
0.2	2.8	0.13	5.0	0.17	7.5	0.20
0.4	5.0	0.27	11.8	0.34	19.5	0.40
0.6	11.0	0.40	21.0	0.51	33	0.60
0.8	18.5	0.54	31.5	0.67	47	0.80
1.0	27.4	0.67	44.0	0.84	61.7	1.00
1.2	37.3	0.81	55.5	1.01	77.3	1.20
1.4	48.5	0.94	70.5	1.18	96	1.40
1.6	59.8	1.08	85.0	1.35	115.4	1.60
1.8	71.0	1.21	101.0	1.52	136.5	1.80
2.0	81.5	1.35	115.0	1.69	155	2.00
2.2	91.5	1.48	129.2	1.85	173.7	2.20
2.35	97.0	1.58	137.2	1.98	185.5	2.35

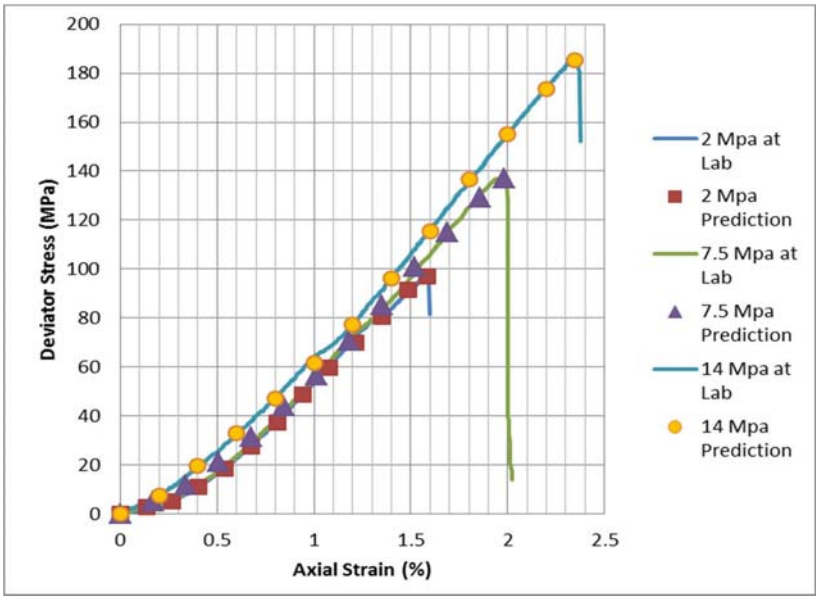

Figure 9. Predicted stress-strain curves plotted superimposed on the actual laboratory stress-strain curves.

The predicted stress and strain magnitudes for confining pressures of 2 MPa, 7.5 MPa and 14 MPa are as being presented in Table 2 and have been plotted as stress-stress data points in Figure 9. The line graphs are the stress-strain curves obtained from the triaxial tests at confining pressures of 2 MPa, 7.5 MPa and 14 MPa. A very close predicted stress-strain response has been achieved in comparison

with the graphs obtained from the laboratory triaxial tests. This is the advantage of incorporating both deformation driving and resisting variables in the deformation framework. Besides, the framework is derived from the actual stress-strain behaviour.

The procedure deployed by this rock deformation framework for predicting the rock stress-strain response is summarized as follows;

i. Conducting rock triaxial tests for at least three different confining pressures to determine the test rock stress-strain curves.
ii. Plot the rock stress-strain curves.
iii. Determine the maximum axial strain at failure from the stress-strain curves.
iv. Obtain normalised stress-strain curves by multiplying the respective axial strains with respective normalise factor so that all peak failure deviator stresses is shifted to coincide with the maximum failure axial strain. (refer Figure 5)
v. Decide the increment of axial strain from 0% to failure, so that the mobilised shear strength envelopes could be drawn based on this increment.
vi. Draw the Mohr circles corresponding to each axial strain under consideration.
vii. Draw the mobilised shear strength envelopes corresponding to each axial strain under consideration.
viii. Once all of the mobilised shear strength have been drawn, the Mohr circles need to be removed. These envelopes are then considered as the inherent property of the test rock, and will be utilized for the prediction of deviator stress for any confining pressure. (Figure 7)
ix. A mobilised shear strength envelope is representing a certain value of axial strain.
x. To predict the magnitude of deviator stress corresponding to a certain axial strain a Mohr circle is drawn to touch the corresponding mobilised shear strength envelope with the minor principle stress, σ_3 representing the applied confining pressure. (Figure 8a, 8b, 8c)
xi. The resulted diameter of the Mohr circle represents the deviator stress corresponding to the axial strain considered.
xii. This process is repeated for all considered mobilised shear strength envelopes and the relationship between the deviator stress and the corresponding axial strain can be plotted to represent the stress-strain relationship for the confining pressure under consideration.
xiii. This process can be repeated for other confining pressure and the stress-strain curve can be determined.
xiv. The normalised strain values need to be converted to actual axial strain by multiplying with the normalised inverse factor as obtained in Equation 2. (Data as in Table 2)
xv. Plot the graph using the inversed axial strain versus the predicted deviator stress. In this manner the predicted stress-strain curves can be obtained. (refer Figure 9)

6. Conclusions

In this paper, a state-of-the-art theoretical method for anisotropic rock deformation model has been introduced. The model applies the rock true stress-strain curves to derive the development of mobilised shear strength whenever the rock is subjected to anisotropic compression. The relationship between the position of the mobilised shear strength envelopes and the corresponding axial strain is considered as a unique rock mass inherent property and this property is used to predict the rock stress-strain response under anisotropic stress condition. The position of the mobilised shear strength envelopes is identified base on the mobilised minimum friction angle. This inherent mobilised shear strength essentially increases when the rock is subjected to anisotropic compression and this can be seen as the envelope rotates upwards towards the shear strength envelope at failure. By this manner the mobilised shear strength is incorporated in characterising the rock deformation with respect to the applied stress.

The following conclusions can be drawn from this study;

i. Currently there is no theoretical framework to predict rock stress-strain response under anisotropic stress condition.

ii. This anisotropic rock deformation model is the first rock theoretical framework that can predict the rock stress-strain response.
iii. The predicted stress-strain response has close agreement compared to the laboratory stress-strain curves as shown in Figure 9. This substantiates the validity of this rock volume change framework.
iv. The applicability of this theoretical framework for other rocks needs to be tested.

Acknowledgements
The work in this paper was performed at the Department of Civil Engineering, Universiti Teknologi Mara, Shah Alam, Malaysia. The authors are thankful for the co-operation between the Department of Civil Engineering, Universiti Teknologi Mara, Kota Samarahan, Sarawak, Malaysia and the Department of Civil Engineering, Universiti Teknologi Mara, Shah Alam, Malaysia, for their support.

7. References

[1] Yang J P, Chen W Z, Yang D S and Yuan J Q 2015 Numerical determination of strength and deformability of fractured rock mass by FEM modeling *Computers and Geotechnics* **64** pp 20-31
[2] Xu Y H and Cai M 2016 Numerical study on the influence of crosssectional shape on strength and deformation behaviors of rocks under uniaxial compression *Computers and Geotechnics* **84** pp 129–137
[3] Cheng C, Chen X and Zhang S 2016 Multipeak deformation behavior of jointed rock mass under uniaxial Compression: Insight from particle flow modeling *Engineering Geology* **213** pp 25-45
[4] Korneva I, Tondi E, Balsamo F and Agosta F 2016 Deformation mechanisms and petrophysical properties of chert and limestone fault rocks within slope to basin succession (Gargano Promontory, Southern Italy) *Tectonophysics* **690** Part A pp 52-62
[5] Xue L, Qin S, Sun Q, Wang Y and Qian H 2014 A quantitative criterion to describe the deformation process of rock sample subjected to uniaxial compression: From criticality to final *Physica A: Statistical Mechanics and its Applications* **410** pp 470-482
[6] Wang S Y, Sloan S W, Sheng D C, Yang S Q and Tang C A 2014 Numerical study of failure behaviour of precracked rock specimens under conventional triaxial compression *International Journal of Solids and Structures* **51** pp 1132–1148
[7] Li J, Hu M, Ding E, Kong W, Pan D and Chen S 2016 Multiparameter numerical simulation of dynamic monitoring of rock deformation in deep mining *International Journal of Mining Science and Technology* **26** Issue 5 pp 851–855
[8] Md Noor M J and Anderson W F 2006 A comprehensive shear strength model for saturated and unsaturated soils Proc. 4th Int. Conf. on Unsaturated Soils **2** pp 1992-2003
[9] Md Noor M J and Anderson W F 2015 Concept of effective stress and shear strength interaction in rotational multiple yield surface framework and volume change behaviour of Banting Clay *Proc. of the Int. Conf. on Applied and Theoretical Mechanics* **11** pp 159-168
[10] Hoek E and Brown E T 1980 Empirical strength criterion for rock masses *A.S.C.E. Journal of Geotechnical Engineering Division* **106** pp 1013-1035